

UNCLASSIFIED

AD 401 818

*Reproduced
by the*

DEFENSE DOCUMENTATION CENTER

FOR

SCIENTIFIC AND TECHNICAL INFORMATION

CAMERON STATION, ALEXANDRIA, VIRGINIA



UNCLASSIFIED

NOTICE: When government or other drawings, specifications or other data are used for any purpose other than in connection with a definitely related government procurement operation, the U. S. Government thereby incurs no responsibility, nor any obligation whatsoever; and the fact that the Government may have formulated, furnished, or in any way supplied the said drawings, specifications, or other data is not to be regarded by implication or otherwise as in any manner licensing the holder or any other person or corporation, or conveying any rights or permission to manufacture, use or sell any patented invention that may in any way be related thereto.

⑤-96160

⑥ A METHOD of NUMERICALLY EVALUATING the ERRORS RESULTING
from MEASUREMENT of SPECIFIC SHOCK IMPULSES by ACCELEROMETERS
due to the FREQUENCY RESPONSE CHARACTERISTICS of the ACCELEROMETER

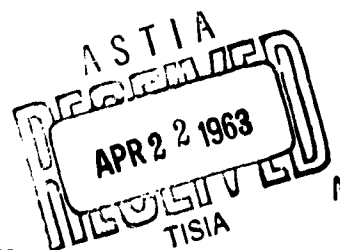
by

⑦ Richard H. Jessen
Captain, USAF

⑧ N.A.
⑨ 14 p. incl. illus.
⑩ N.A.
⑪ N.A.
⑫ N.A.
⑬ N.A.

Plan B Paper

Submitted to the Department of
Mechanical Engineering and the Graduate
School of the University of Wyoming in Partial
Fulfillment of Requirements for the Degree of
Master of Science



University of Wyoming

Laramie, Wyoming

⑭ Jan 1963

ACKNOWLEDGEMENT

The author wishes to express his sincere appreciation to Dr. J. E. Foster, Department of Mechanical Engineering, University of Wyoming, for his guidance and assistance in the preparation of this paper.

TABLE OF CONTENTS

CHAPTER	PAGE
I INTRODUCTION	1
II SHOCK INPUTS TRANSFORMED TO THE FREQUENCY DOMAIN	4
SQUARE WAVE SHOCK PULSE	5
HALF SINE WAVE SHOCK PULSE	6
TRIANGULAR WAVE SHOCK PULSE	9
III INDUCED ERROR DUE TO THE FREQUENCY RESPONSE LESS THAN UNITY	11
ERROR CALCULATION RESULTS	14
IV CONCLUSIONS	15
APPENDIX	16

LIST OF FIGURES

FIGURE	PAGE
1. Frequency Response Curve of a Conventional Crystal Accelerometer	2
2. Input and Output Wave Forms for Accelerometer with Frequency Response Less than Unity in the Low Frequency Range	3
3. Square Wave Shock Pulse	5
4. Half Sine Shock Pulse	6
5. Triangular Shock Pulse	9
6. Product (Curve C) of the Frequency Spectrum (Curve A) for a 10 Millisecond Square Pulse and Frequency Response (Curve B) of the Accelerometer	11
7. Frequency Curve Divided into Small Incremental Areas . . .	12
8. Frequency Response Curve for Endevco Model Accelerometer (Capacitance 500mmfd and Impedance 100megohms)	13

CHAPTER I

INTRODUCTION

Vibration and shock have become important fields of mechanical engineering with the advent of high speed aircraft and missiles. The equipment or "black boxes" installed in today's air vehicles are subjected to rigorous vibration inputs and sudden shock forces and must be designed to operate or at least withstand these conditions. Vibration can be defined in terms of displacement, velocity, and acceleration while shock is generally defined as a change in velocity which gives rise to high accelerations. Acceleration is the value most often desired because the destructive force is proportional to the mass times the indicated acceleration. Many times knowledge of the destructive force is a desirable quantity and if the indicated acceleration cannot be accurately determined the calculated force will be of little or no value. Factors such as mounting techniques, temperature effects, acoustical effects, calibration errors, and frequency response all affect the accuracy of the recorded environmental data. The effect of the frequency response upon the accuracy of the acceleration data will be the main factor discussed in this paper.

The type of transducer most frequently used for vibration and shock measurement is a crystal or piezoelectric accelerometer. The ability of certain crystalline material to generate a charge when subjected to a physical stress has been known for many years. Some of the common crystalline materials are: Rochelle Salt, Quartz, Barium Titanate, Lead

Zirconate-Lead Titanate and Lead Metaniobate. When the accelerometer is subjected to an input a mechanical strain is applied to the crystal. The stress in the crystal causes very small displacements of the crystal domain which generates a charge on opposite surfaces. A crystal deflection of three micro-inches may produce as much as 100 volts.

The input to be considered in this paper will be a shock rather than a vibration input. The shock inputs most frequently associated with the airframe and missile field, insofar as environmental testing, are a 10 millisecond square wave shock pulse, 10 millisecond half sine wave shock pulse, and the seven millisecond triangular shock pulse.

The ability of the transducer to faithfully reproduce an input is related to the frequency response of the accelerometer. A typical response curve for a crystal accelerometer is shown in Figure 1.

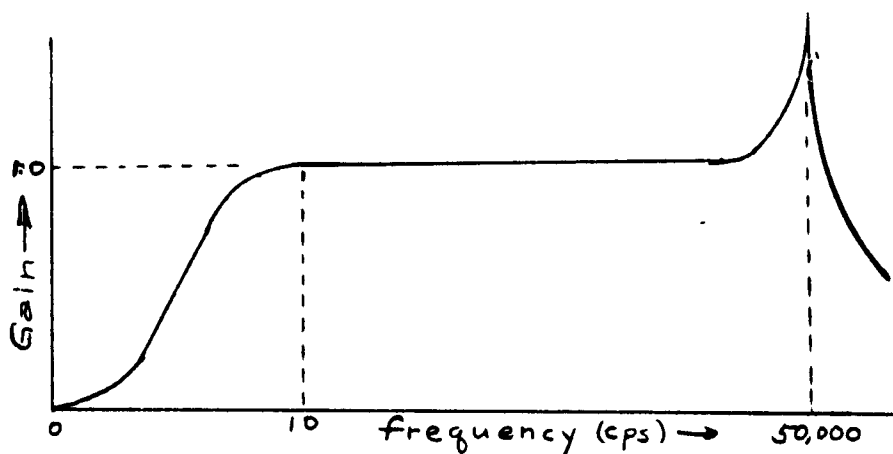


Fig. 1
Frequency Response Curve of a
Conventional Crystal Accelerometer

The response of a crystal accelerometer (Fig. 1) with respect to frequency has a useful region called the mid-band range, where the gain is independent of frequency. Above and below this mid-band region the gain is dependent upon the frequency. For this reason it is always desirable to operate the accelerometer at frequencies within this mid-band range. The question then arises as to how satisfactory the accelerometer data would be for certain types of shock excitation where the frequency content of the pulse could be below the mid-band range. For example, if the frequency content is below the mid-band range (gain less than unity) and the input is a square wave the output of the accelerometer will not be a "square" square wave (Fig. 2). In this example the accelerometer would not be faithfully reproducing the input.

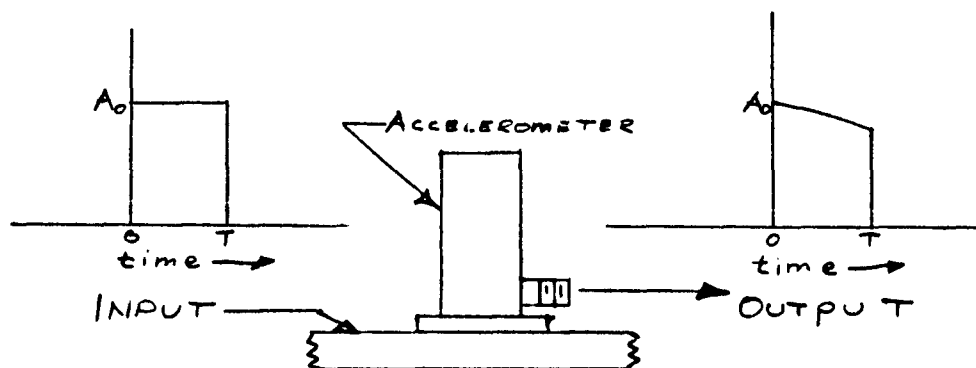


Fig. 2
Input and Output Wave Forms for Accelerometer with Frequency
Response less than Unity in the Low Frequency Range.

This paper will present a method of calculating the error of a crystal accelerometer due to its frequency response being less than unity in the low frequency range. The inputs considered will be the three types of shock pulses previously mentioned.

CHAPTER II

SHOCK INPUTS TRANSFORMED TO THE FREQUENCY DOMAIN

The shock input is a function of time (nonperiodic) " $F(t)$ " and must be transformed into a function of frequency " $F(f)$ ". This is necessary to determine what effect the frequency response of the accelerometer will have on the input signal. The mathematical tool which is used to transform from the time domain to the frequency domain is the Fourier Integral (Equation 1.1)¹. This equation is analogous to the Fourier Series which is used for a periodic input function.

$$F(\omega) = \int_{-\infty}^{\infty} F(t) \cdot e^{-j\omega t} \cdot dt \quad \text{Eq. 1.1}$$

This mathematical tool will enable the engineer to determine the frequency content of any nonperiodic pulse, by this it is meant, the number of frequencies which must be summed to duplicate the pulse.

The frequency range of most crystal accelerometers is 3-50,000 cps however many amplifiers associated with the accelerometer have a range of 0-10,000 cyps. It is recognized that there are a number of suitable amplifiers whose range may well exceed 50,000 cps, however shock measurements are primarily associated with the low frequencies and this paper will deal only with frequencies between 0-10,000 cps.

¹Van Valkenburge, M. E., NETWORK ANALYSIS, Prentice-Hall Inc., Englewood Cliffs, N. J., 1955, p.185.

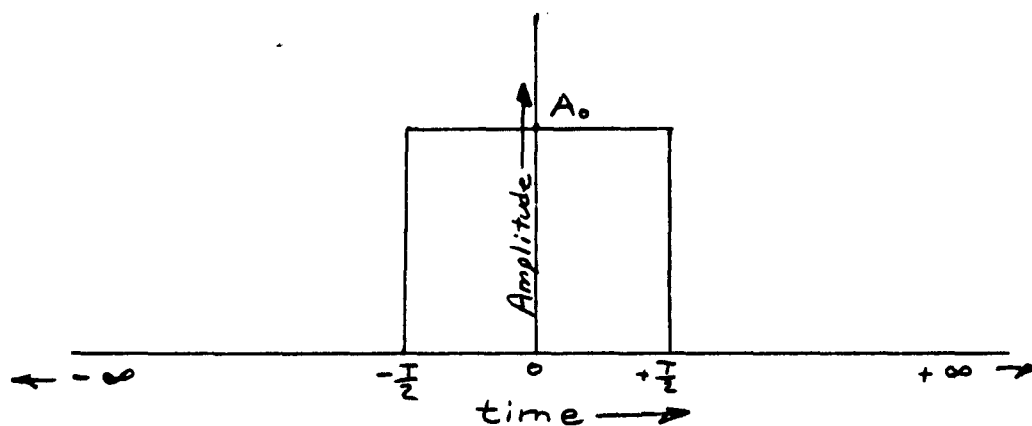
SQUARE WAVE SHOCK PULSE

Fig. 3
Square Wave Shock Pulse

The time function of a square wave (Fig. 3) is given by

$$F(t) = A_0 \quad - \quad \frac{T}{2} \leq t \leq \frac{T}{2} \quad \text{Eq. 2.1}$$

and

$$F(t) = 0 \quad \text{everywhere else}$$

where "T" is the period of duration of the pulse. Substituting $F(t) = A_0$ into Equation 1.1, $F(f)$ is given by

$$F(\omega) = \int_{-\infty}^{-\frac{T}{2}} 0 \cdot e^{-j\omega t} dt + \int_{-\frac{T}{2}}^{\frac{T}{2}} A_0 \cdot e^{-j\omega t} dt + \int_{\frac{T}{2}}^{\infty} 0 \cdot e^{-j\omega t} dt$$

$$F(\omega) = -\frac{A_0}{j} (e^{-j\omega t}) \Bigg|_{-\frac{T}{2}}^{\frac{T}{2}}$$

$$F(\omega) = \frac{2 A_0}{\omega} \left(\frac{e^{j\omega \frac{T}{2}} - e^{-j\omega \frac{T}{2}}}{2j} \right)$$

$$F(\omega) = \frac{2 A_0}{\omega} \sin \frac{\omega T}{2} \quad \text{Eq. 2.2}$$

Substituting $\omega = 2\pi f$ and rearranging terms, the final form of Eq. 2.2 is

$$F(f) = A_0 \frac{T}{2\pi} \left(\frac{\sin \pi f t}{\pi f t} \right) \quad \text{Eq. 2.3}$$

where "f" is the frequency in cycles per second (cps).

Equation 2.3 is the equation for the frequency spectrum curve for a square wave shock pulse of duration "T". The graph of Equation 2.3 is shown in Fig. A-1.

HALF SINE WAVE SHOCK PULSE

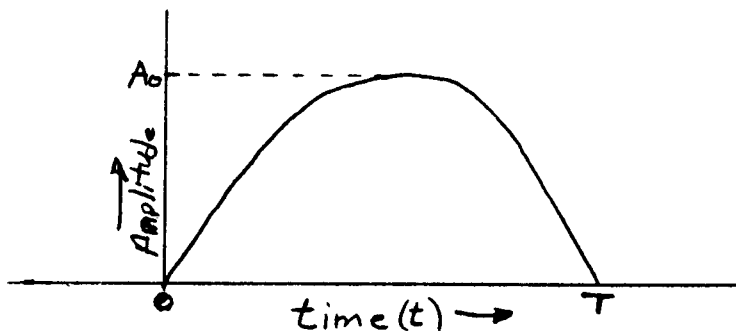


Fig. 4
Half Sine Shock Pulse

The time function $F(t)$ for a sine wave (Fig. 4) is $A_0 \sin \frac{\pi t}{T}$ between 0 and T and zero (0) everywhere else. The frequency spectrum for a half sine wave is obtained by again using Equation 1.1 as follows:

$$F(\omega) = \int_{-\infty}^{\infty} F(t) e^{-j\omega t} dt$$

$$F(\omega) = \int_0^T A_0 \sin \frac{\pi t}{T} e^{-j\omega t} dt$$

$$F(\omega) = A_0 \int_0^T \left(\frac{e^{j\frac{\pi}{T}t} - e^{-j\frac{\pi}{T}t}}{2j} \right) e^{-j\omega t} dt$$

$$F(\omega) = \frac{A_0}{2j} \int_0^T \left(e^{j(\frac{\pi}{T} - \omega)t} - e^{-j(\frac{\pi}{T} + \omega)t} \right) dt$$

$$F(\omega) = \frac{A_0}{2j} \left[\frac{e^{j(\frac{\pi}{T} - \omega)t}}{j(\frac{\pi}{T} - \omega)} + \frac{e^{-j(\frac{\pi}{T} + \omega)t}}{j(\frac{\pi}{T} + \omega)} \right]_0^T$$

$$F(\omega) = \frac{A_0}{2j} \left(\frac{e^{j(\frac{\pi}{T} - \omega)T} - 1}{j(\frac{\pi}{T} - \omega)} + \frac{e^{-j(\frac{\pi}{T} + \omega)T} - 1}{j(\frac{\pi}{T} + \omega)} \right)$$

$$F(\omega) = \frac{A_0}{2j} \left(\frac{(\frac{\pi}{T} + \omega)(e^{j\pi} \cdot e^{-j\omega T} - 1) + (\frac{\pi}{T} - \omega)(e^{-j\pi} \cdot e^{-j\omega T} - 1)}{j(\frac{\pi}{T} - \omega)(\frac{\pi}{T} + \omega)} \right)$$

$$F(\omega) = \frac{A_0}{2j} \frac{\frac{2\pi}{T} (\cos \pi) e^{-j\omega T} + 2\omega j (\sin \pi) e^{-j\omega T} - \frac{2\pi}{T}}{j \left(\left(\frac{\pi}{T} \right)^2 - \omega^2 \right)}$$

$$F(\omega) = \frac{A_0}{2j} \left(\frac{-\frac{2\pi}{T} e^{-j\omega T} - \frac{2\pi}{T}}{j \left(\left(\frac{\pi}{T} \right)^2 - \omega^2 \right)} \right)$$

$$F(\omega) = \frac{A_0 \pi}{T} \left(\frac{1 + e^{-j\omega T}}{\left(\frac{\pi}{T}\right)^2 - \omega^2} \right)$$

$$F(\omega) = \frac{A_0 \pi T^2}{T} \frac{1 + \cos \omega T - j \sin \omega T}{\pi^2 - (T\omega)^2}$$

$$F(\omega) = \frac{A_0 \pi T}{\pi^2 - (T\omega)^2} (1 + \cos \omega T - j \sin \omega T)$$

The phase shift will be neglected because the magnitude of the frequency content is the primary factor in this paper. Therefore,

$$F(\omega) = \frac{A_0 \pi T}{\pi^2 - (T\omega)^2} \sqrt{(1 + \cos \omega T)^2 + (\sin \omega T)^2}$$

$$F(\omega) = \frac{A_0 \pi T}{\pi^2 - (T\omega)^2} \sqrt{2 + 2 \cos \omega T}$$

$$F(\omega) = \frac{A_0 \pi T \sqrt{2}}{\pi^2 - (T\omega)^2} \sqrt{1 + \cos \omega T}$$

$$F(\omega) = \frac{A_0 \pi T}{\pi^2 - (T\omega)^2} \cos \frac{\omega T}{2} \quad \text{Eq. 2.4}$$

Substituting $\omega = 2\pi f$ into equation 2.4 and rearranging terms the final form is

$$F(f) = \frac{A_0 T}{2\pi^2} \frac{\cos \pi f T}{1 - 4f^2 T^2} \quad \text{Eq. 2.5}$$

Equation 2.5 is the equation for the frequency spectrum curve for a half sine wave shock pulse of duration "T". The graph of Equation 2.5 is shown in Fig. A-2.

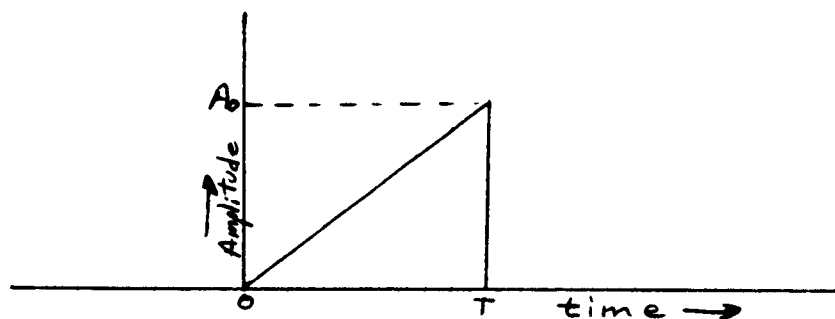
TRIANGULAR WAVE SHOCK PULSE

Fig. 5
Triangular Shock Pulse

The time function of a triangular wave shock pulse (Fig. 6) is

$$F(t) = \frac{A_0}{T} t \quad 0 \leq t \leq T \quad \text{Eq. 2.6}$$

and

$$F(t) = 0 \quad \text{everywhere else.}$$

Substituting Equation 2.6 into the transform Equation 1.1 the resulting frequency spectrum equation is given by

$$F(\omega) = \int_0^T \frac{A_0}{T} t e^{-j\omega t} dt$$

$$F(\omega) = \frac{A_0}{T} \left[\frac{t e^{-j\omega t}}{-j\omega} \right]_0^T + \frac{1}{j} \int_0^T e^{-j\omega t} dt$$

$$F(\omega) = \frac{A_0}{T} \frac{T e^{-j\omega T}}{-j\omega} + \left(\frac{1}{j\omega} \right)^2 (e^{-j\omega T} - 1)$$

$$F(\omega) = \frac{A_0}{\omega T} \left[\frac{1}{\omega} (e^{-j\omega T} - 1) - T e^{-j\omega T} \right]$$

$$F(\omega) = \frac{A_0}{\omega T} \left[\left(\frac{1}{\omega} + j T \right) e^{-j\omega T} - \frac{1}{\omega} \right]$$

$$F(\omega) = \frac{A_0}{\omega T} \left[\left(\frac{1}{\omega} + j T \right) (\cos \omega T - j \sin \omega T) - \frac{1}{\omega} \right]$$

$$F(\omega) = \frac{A_0}{\omega T} \left\{ \frac{1}{\omega} [(\cos \omega T - 1) + T \sin \omega T] + j(T \cos \omega T - \frac{1}{\omega} \sin \omega T) \right\}$$

Again neglecting phase shift

$$F(\omega) = \frac{A_0}{\omega T} \sqrt{\left[\frac{1}{\omega} (\cos \omega T - 1) + T \sin \omega T \right]^2 + \left[T \cos \omega T - \frac{1}{\omega} \sin \omega T \right]^2}$$

$$F(\omega) = \frac{A_0}{\omega T} \sqrt{\frac{1}{\omega^2} - \frac{2}{\omega^2} \cos \omega T + T^2 + \frac{1}{\omega^2} - \frac{2T}{\omega} \sin \omega T}$$

$$F(\omega) = \frac{A_0 \sqrt{2} T}{\omega^2 T^2} \sqrt{1 + \frac{\omega^2 T^2}{2} - \cos \omega T - \omega T \sin \omega T}$$

$$F(\omega) = \frac{A_0 T \sqrt{2}}{\omega^2 T^2} \sqrt{1 + \frac{\omega^2 T^2}{2} - (\cos \omega T + \omega T \sin \omega T)} \quad \text{Eq. 2.7}$$

Substituting $\omega = 2\pi f$ the final form is

$$F(f) = \frac{A_0 T \sqrt{2}}{2\pi(2\pi f T)^2} \sqrt{1 + \frac{(2\pi f T)^2}{2} - (\cos 2\pi f T + 2\pi f T \sin 2\pi f T)} \quad \text{Eq. 2.8}$$

Equation 2.8 is the equation for the frequency spectrum curve for a triangular wave shock pulse of duration "T". The graph of Equation 2.8 is shown in Figures A-3 and A-4.

CHAPTER III

INDUCED ERROR DUE TO THE FREQUENCY RESPONSE BEING LESS THAN UNITY

In Chapter II the three types of shock inputs were transformed into the frequency domain and the resulting frequency equations were plotted in Figures A-1, A-2, A-3, and A-4. The absolute areas bounded by these curves are used to determine the induced error. At the low frequencies the response of the accelerometer is less than unity, therefore, those frequencies in the input signal in the low range will be distorted by the transducer. This means the absolute area under the frequency spectrum curve at the transducer output is less than at the input. The curve at the output is the product of the frequency spectrum of the input pulse times the frequency response of the accelerometer (Fig. 7).

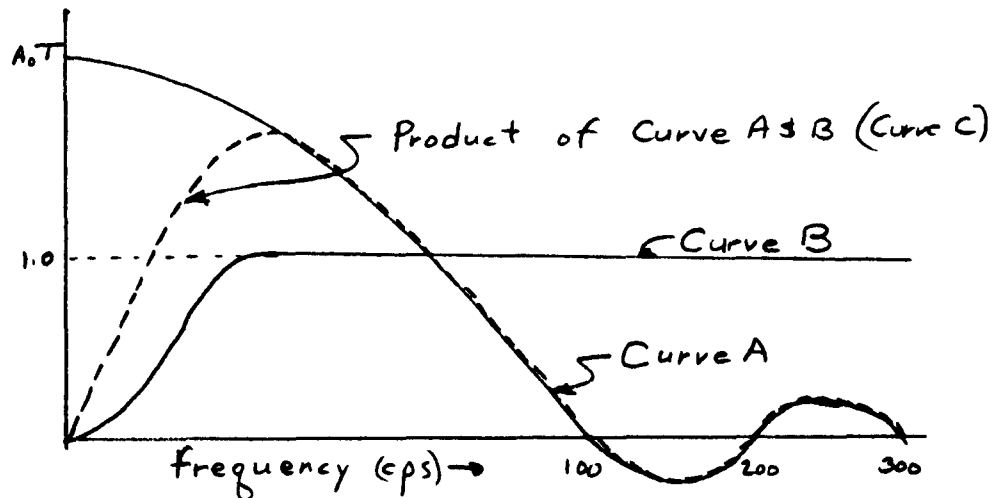


Fig. 6
Product (Curve C) of the Frequency Spectrum (Curve A) for a
10 Millisecond Square Pulse and Frequency Response
(Curve B) of the Accelerometer

The calculated percentage error as used in the paper is given by

$$\% \text{ error} = 100 \frac{(\text{area under curve A}) - (\text{area under curve C})}{(\text{area under curve A})}$$

The transducer that was chosen as a typical piezoelectric accelerometer was the Endevco model 2213 manufactured by the Endevco Corporation, 161 East California Boulevard, Pasadena, California. The frequency response (Fig. 8) for the unit is based on a total capacitance of 500 mmfd (accelerometer and cable) and an amplifier input impedance of 100 megohms. The response is flat (unity gain) above 40 cps.

For all curves the bounded area is found by integrating the equation for the frequency spectrum curve (2.3) between zero and 10,000 cps. This integration was accomplished on the Bendix G-15D digital computer by using Trapezoidal Rule which is the numerical integration or addition of small incremental areas along the frequency axis. The general form is

$$\left(\frac{y_i + y_{i+1}}{2} \right) (\Delta f)$$

where y_i and y_{i+1} are the heights above the frequency axis and Δf is the frequency increment along the axis (Fig. 7).

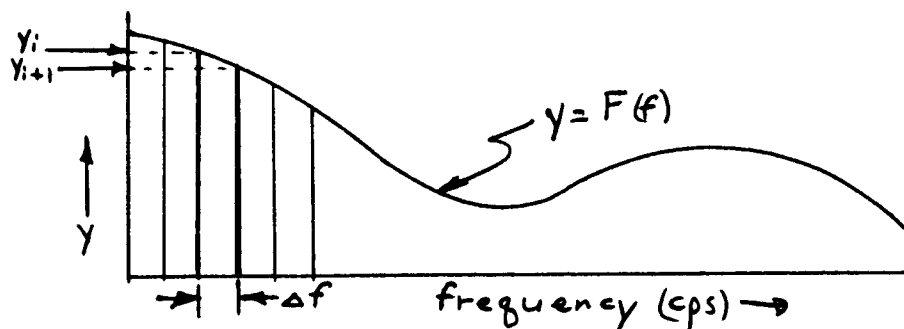


Fig. 7:
Frequency Curve Divided into Small Incremental Areas

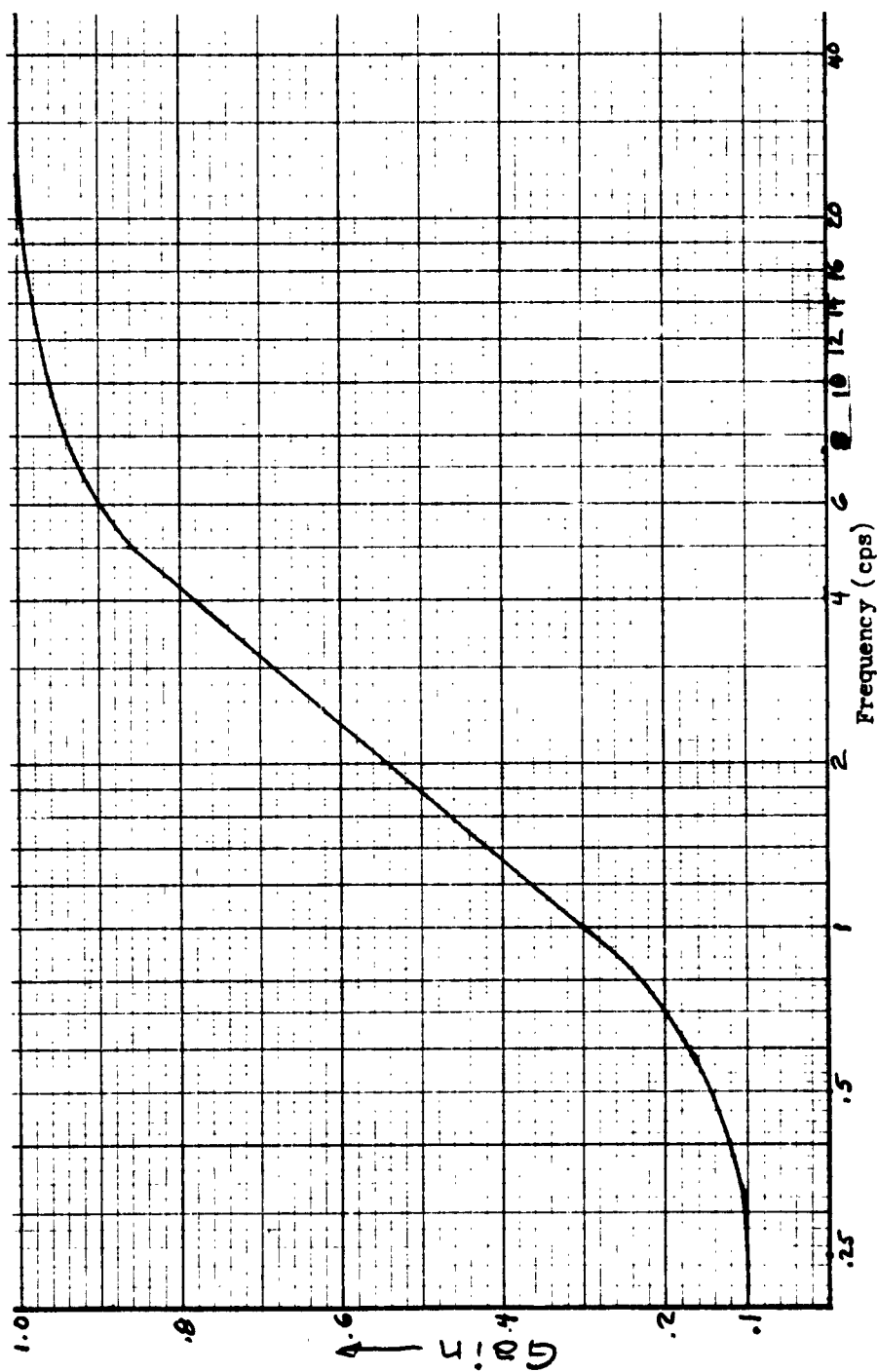


Fig 8
Frequency Response Curve for Endevco Model 2213 Accelerometer
(Capacitance 500mmfd and Impedance 100megohms)

ERROR CALCULATION RESULTS

For a square pulse the computed area is $1.501860 (A_0)$ using increments of .25 cps between 0.25 and 25 cps, 5 cps between 25 and 3,000 cps, and 20 cps between 3,000 and 10,000 cps. The loss in area due to the frequency response being less than unity below 25 cps is $0.027238 (A_0)$. This is the difference between the total area and the total area as a result of distortion. The area with distortion is the summation of the incremental areas times the gain factor for each respective frequency. The percentage error for the 10 millisecond square wave shock pulse is

$$100 \left(\frac{0.027238 (A_0) (\text{loss in area})}{1.501860 (A_0) (\text{total area})} \right) = 1.8145\% .$$

The percentage error for the half sine wave shock pulse of 10 milliseconds duration (using the same approach as for the square wave) is

$$100 \left(\frac{0.034355(A_0) (\text{loss in area})}{0.92572(A_0) (\text{total area})} \right) = 3.7111\% .$$

Likewise the percentage error for a triangular wave shock pulse of seven milliseconds duration is

$$100 \left(\frac{0.084288814(A_0) (\text{loss in area})}{0.83149729(A_0) (\text{total area})} \right) = 9.8988\% .$$

CHAPTER IV

CONCLUSIONS

The accelerometer error due to the frequency response of the Endevco unit is

1.8145% for a 10 millisecond square wave shock pulse,

3.7111% for a 10 millisecond half sine wave shock pulse,

and

9.8988% for a seven millisecond triangular wave shock pulse.

The error for the square wave is small because most of the area under the curve is about 25 cps where the gain is unity. The area under the curve for the half sine wave pulse rapidly decreases for increasing frequency due to the $4f^2t^2$ term in the denominator of Equation 2.5; therefore, the total area for the half sine wave is smaller than for the square wave. However, the areas below 25 cps are nearly the same thereby making a larger error for the half sine wave.

The large error for the triangular wave is due to the fact that most of the area in the low frequency range where the gain is less than unity.

While the results of this paper cannot be used in a quantitative sense, the purpose has been to emphasize this particular source of error. It is generally neglected in practice but as has been shown, it could represent a sizeable amount of distortion.

APPENDIX

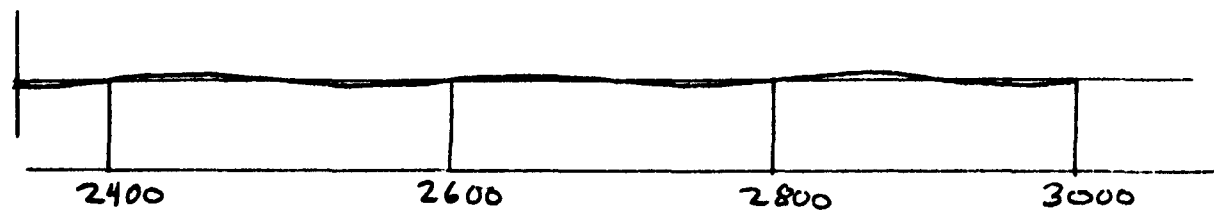
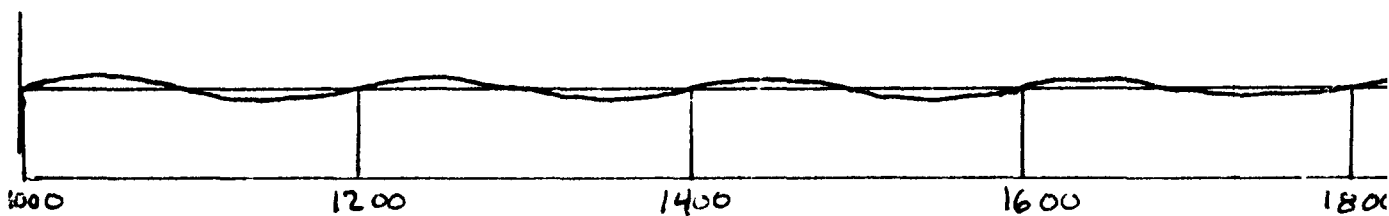
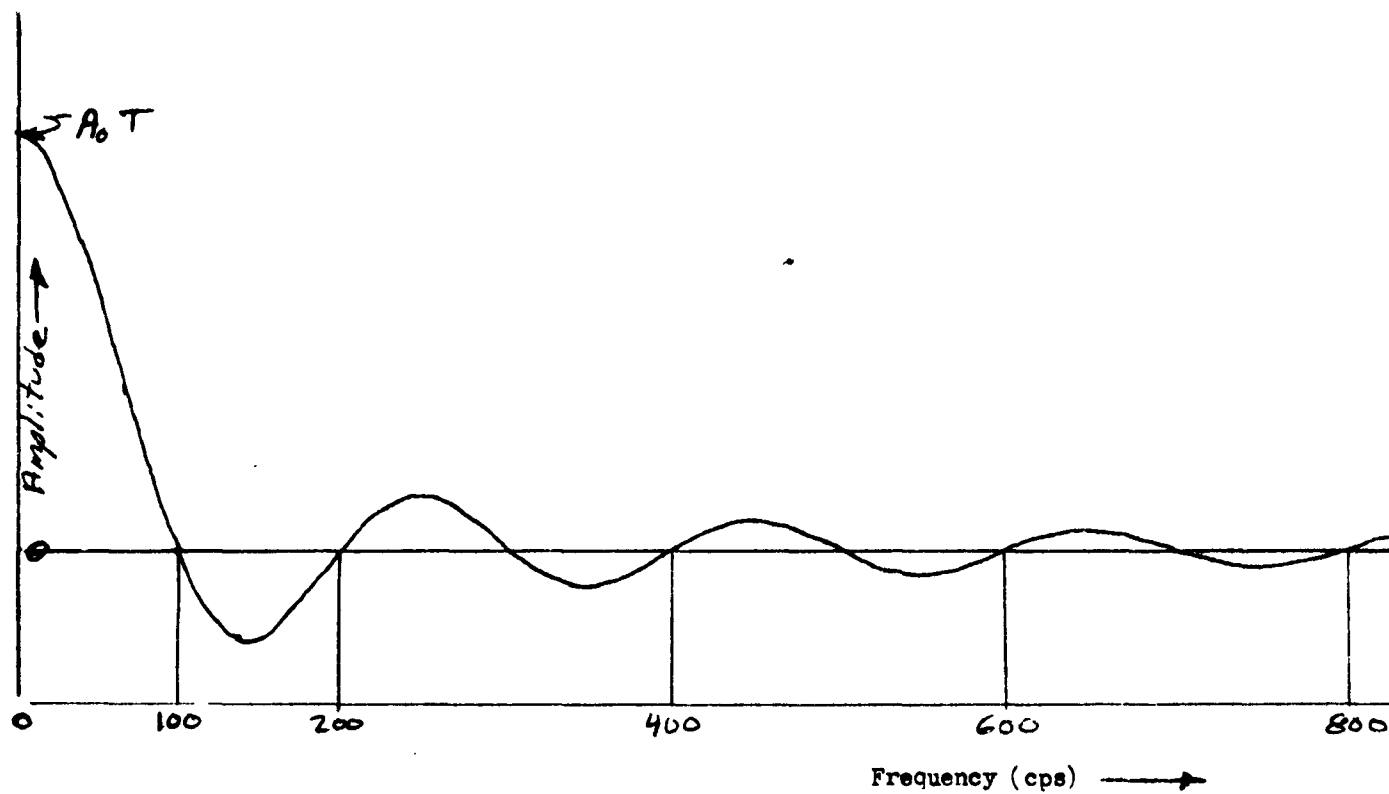


Fig A-1
Frequency Spectrum for a Square Wave Shock Pulse
for a 10 Millisecond Duration

1

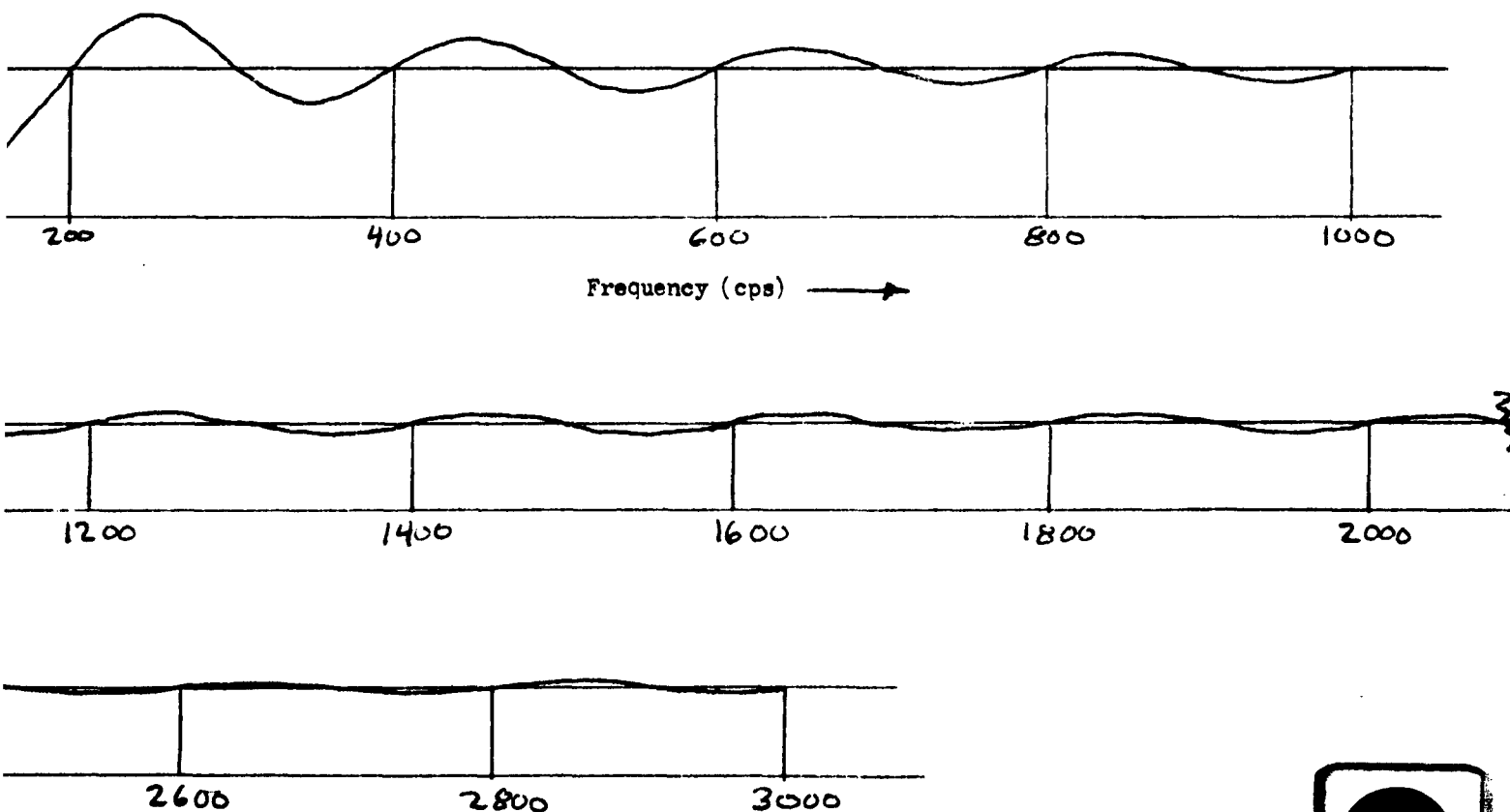


Fig A-1
Frequency Spectrum for a Square Wave Shock Pulse
for a 10 Millisecond Duration

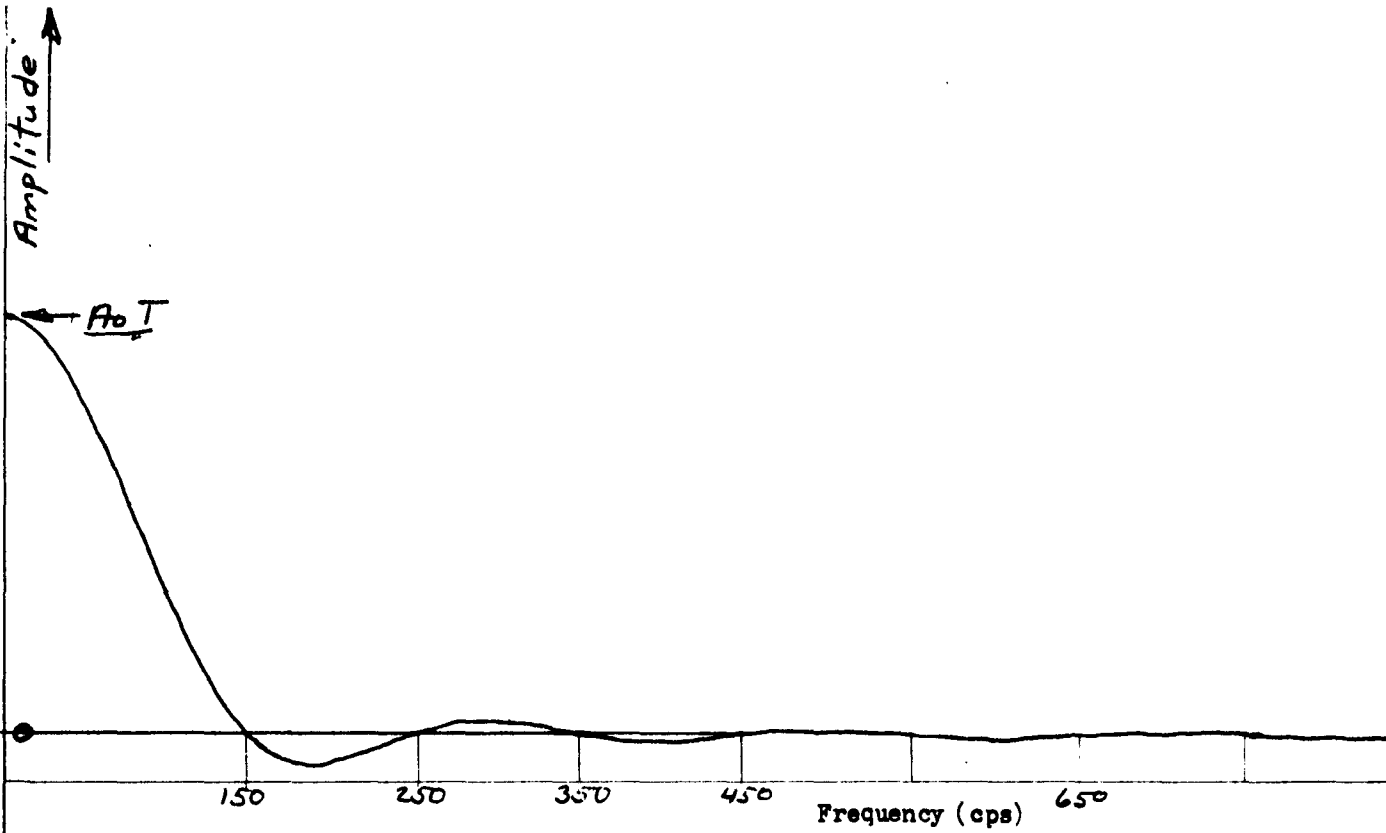


Fig A-2
Frequency Spectrum for a Half Sine Wave Shock Pulse
for a 10 Millisecond Duration

1

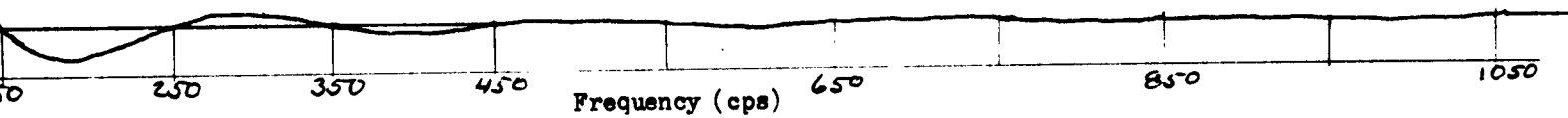


Fig A-2
Frequency Spectrum for a Half Sine Wave Shock Pulse
for a 10 Millisecond Duration

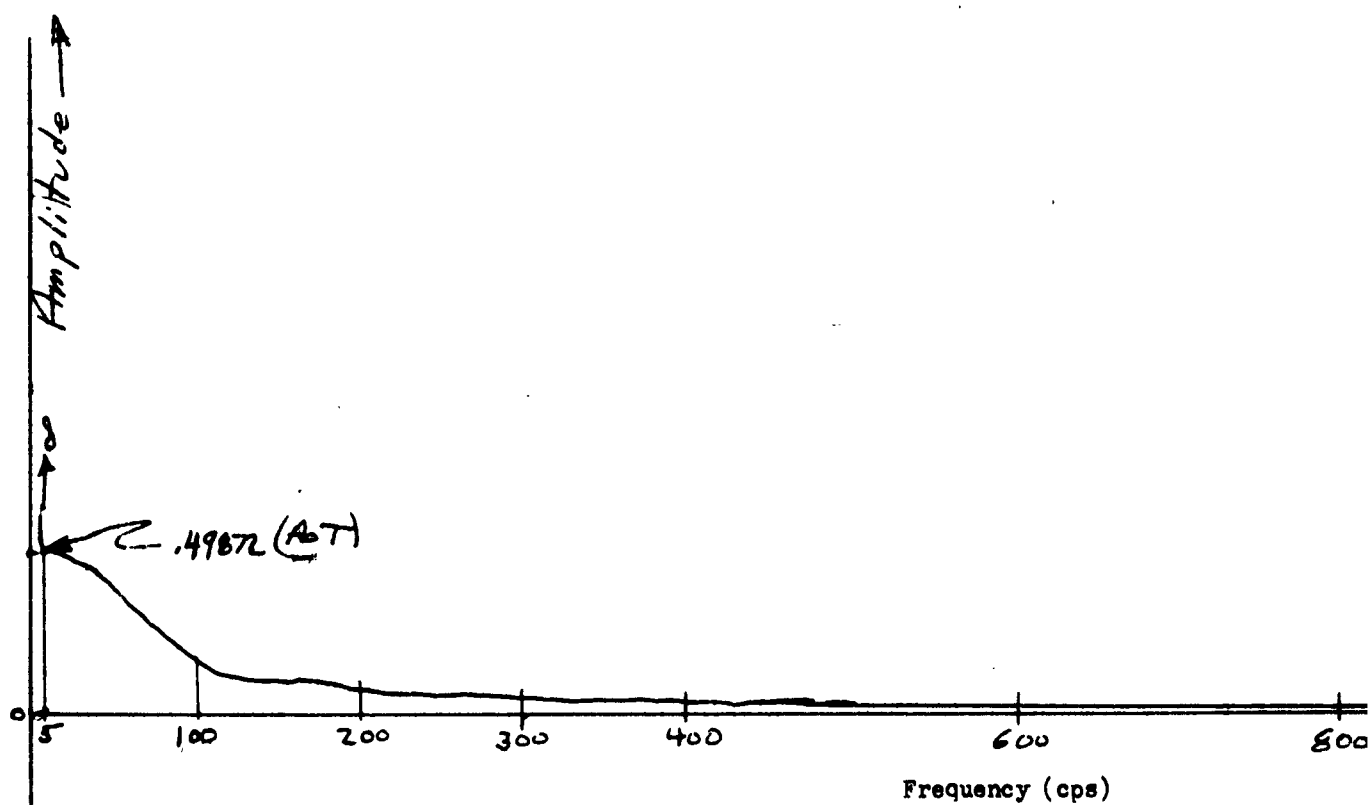


Fig A-3
Frequency Spectrum for a Triangular Wave Shock Pulse
for a 7 Millisecond Duration between 5 and 2,200 cps

1

(AT)

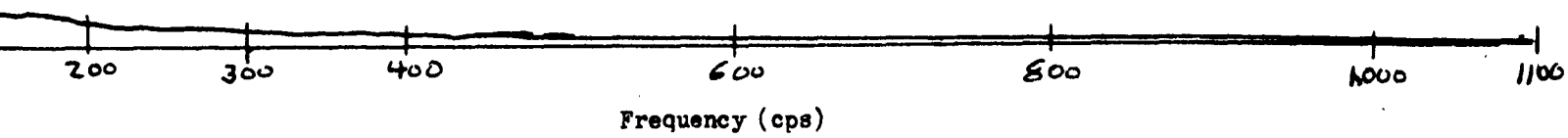


Fig A-3
Frequency Spectrum for a Triangular Wave Shock Pulse
for a 7 Millisecond Duration between 5 and 2,200 cps



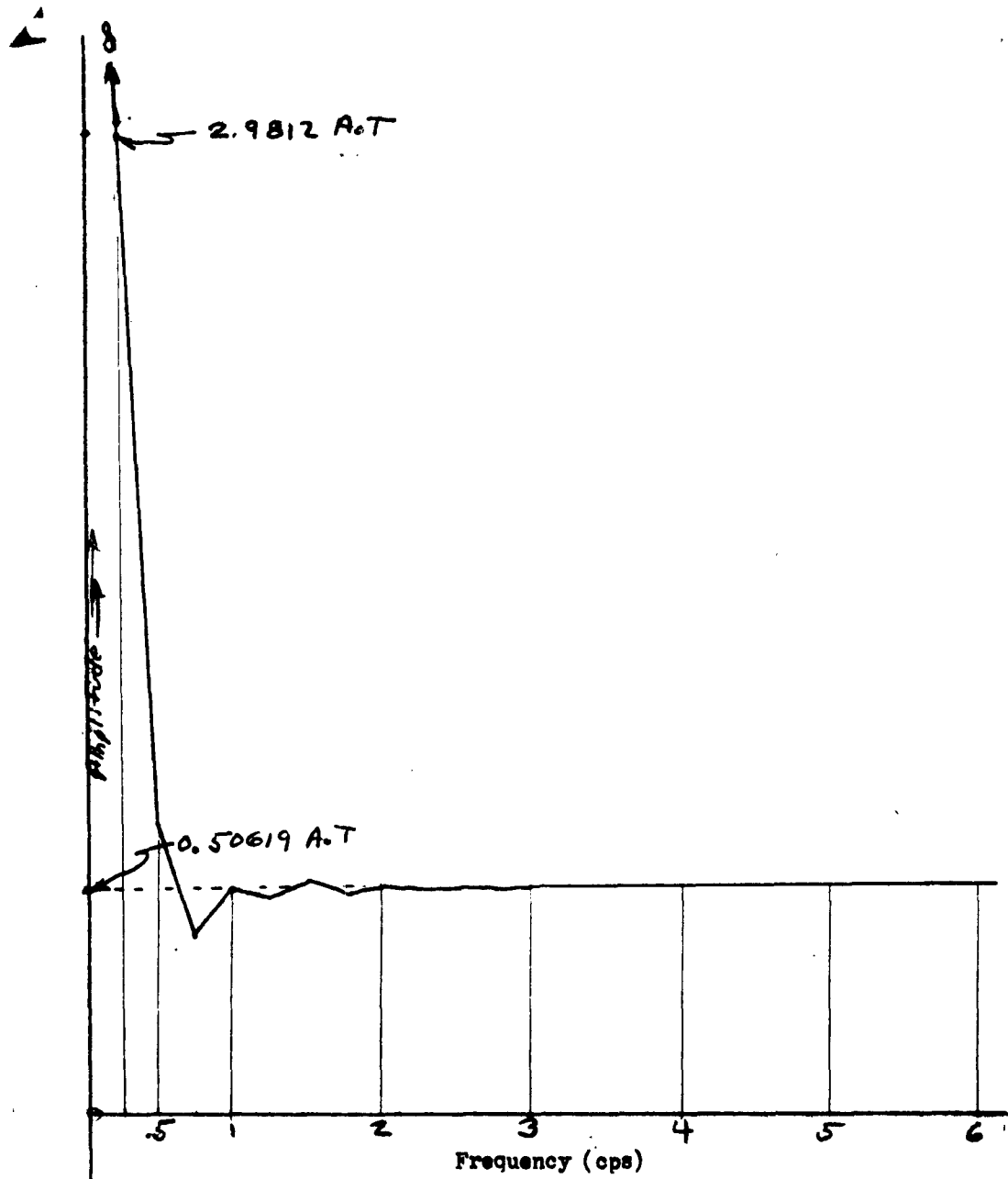


Fig A-4
Frequency Spectrum for a Triangular Wave Shock Pulse
for a 7 Millisecond Duration between 0.25 and 6 cps